Early View

Original research article

Elexacaftor-Tezacaftor-Ivacaftor corrects monocyte microbicidal deficiency in cystic fibrosis

Luca Cavinato, Francesco R. Luly, Valentina Pastore, Daniele Chiappetta, Gloria Sangiorgi, Eva Ferrara, Pia Baiocchi, Giuseppe Mandarello, Giuseppe Cimino, Paola Del Porto, Fiorentina Ascenzioni

Title

Elexacaftor-Tezacaftor-Ivacaftor corrects monocyte microbicidal deficiency in cystic fibrosis

Luca Cavinato[1], Francesco R. Luly[1], Valentina Pastore[1], Daniele Chiappetta[1], Gloria Sangiorgi[1], Eva Ferrara[2], Pia Baiocchi[3], Giuseppe Mandarello[4], Giuseppe Cimino[2], Paola Del Porto[1] and Fiorentina Ascenzioni[1*]

[1]Department of Biology and Biotechnology "Charles Darwin", Sapienza University of Rome, Rome, Italy

[2]Cystic Fibrosis Reference Center of Lazio Region, Policlinico Umberto I, Rome, Italy.

[3]Department of Public Health and Infectious Disease, Sapienza University of Rome, Rome, Italy

[4]Department of Onco-Hematology, Immunotransfusion Service, ASL Viterbo, Italy.

*Corresponding author: Fiorentina Ascenzioni, Department of Biology and Biotechnology "Charles Darwin", Sapienza University of Rome, via dei Sardi 70, 00185 Rome, Italy

Take home message: In people with cystic fibrosis, Elexacaftor-Tezacaftor-Ivacaftor ameliorates the antimicrobial activity of monocytes against *Pseudomonas aeruginosa,* by lowering their exuberant oxidative burst thus contributing to the significant improvement of the lung disease.

Running title: ETI improves antimicrobial activity in Cystic Fibrosis

Total word count: 3408

Key words, CFTR triple-modulators therapy, Monocytes, Phagocytosis, Respiratory burst, *Pseudomonas aeruginosa*, Interleukin-6

Abstract

Question. Cystic Fibrosis (CF), which is caused by mutations in the cystic fibrosis transmembrane conductance regulator (CFTR), is characterized by chronic bacterial lung infection and inflammation. In CF, monocytes and monocyte-derived macrophages have been shown to display defective phagocytosis and antimicrobial activity against relevant lung pathogens, including *Pseudomonas aeruginosa*. Thus, we addressed the effect of the CFTR triple modulator therapy, Elexacaftor/Tezacaftor/Ivacaftor (ETI), on the activity of CF monocytes against *P. aeruginosa*.

Materials/patients and Methods Monocytes from people with CF (PWCF) before and after 1 and 6 months of ETI therapy were isolated from blood and infected with *P. aeruginosa* to assess phagocytic activity and intracellular bacterial killing. The oxidative burst and IL-6 secretion were also determined. Monocytes from healthy controls were also included.

Results and answer to the question Longitudinal analysis of the clinical parameters confirmed an improvement of lung function and lung microbiology by ETI. Both the phagocytic and microbicidal deficiencies of the CF monocytes also improved significantly, although not completely. Furthermore, we measured an exuberant oxidative burst in CF monocytes before therapy, which was reduced considerably by ETI. This led to an improvement of the ROS-dependent bactericidal activity. Inflammatory response to bacterial stimuli was also lowered compared to pre-therapy. PWCF on ETI therapy, in a real-life setting, in addition to clinical recovery, showed significant improvement in monocyte activity against *P. aeruginosa*, which may have contributed to the overall effect of ETI on pulmonary disease. This also suggests that CF monocyte dysfunctions may be specifically targeted to ameliorate lung function in CF.

Introduction

Cystic fibrosis (CF) is a life-limiting genetic disease caused by mutations in the cystic fibrosis transmembrane conductance regulator (*CFTR*) gene with the *F508del* mutation being the most common. In the lung, dysfunctional CFTR causes an imbalance in the ion transport across the airway epithelia, which in turn favors chronic bacterial infections associated with a decline in lung function (1). Extensive structural and functional studies of the wild type and mutated CFTR proteins led to the identification of small molecules, which by interacting with mutated CFTR, restore its activity. CFTR modulators comprise correctors, such as elexacaftor, lumacaftor and tezacaftor, designed to improve misfolded and mistracked CFTR, and potentiators which target gating mutations characterized by the defective opening of the channel pore (2–4). The potentiator, ivacaftor, was the first CFTR corrector to be approved for clinical use, in 2013, in subjects with gating mutations (5, 6). Subsequently, based on the possible synergistic activity of correctors, not only on F508del CFTR but also on other mutant proteins, these drugs were used in combination (7–9) in homozygous and heterozygous people with CF (PWCF) with at least one F508del mutation.

Randomised controlled trials that evaluate the efficacy of CFTR correctors in PWCF with class II mutations, including the *F508del CFTR* allele, have recently been evaluated (10) revealing an improvement in the quality of life (QoL) and lung function for the triple-therapy (elexacaftor-tezacaftor-ivacaftor, ETI), little improvement for the dual therapy (one corrector and one potentiator) while, no relevant effects on lung function were observed for monotherapy (10). Based on the encouraging results obtained with ETI, in October 2019, the U.S. Food and Drug Administration approved this combined therapy for PWCF $\geq$ 12 years old, with at least one *F508del*, followed by the European Medicine Agency in August 2020. Since then, ETI use has significantly increased to the extent that a rapid extension to nearly all eligible PWCF is expected (11–13). It is therefore necessary to extend the study of the

effects of ETI to other cellular districts, other than the epithelia of the airways, which have already been extensively studied.

Monocytes and monocyte-derived macrophages play a key role in maintaining lung sterility and in regulating the inflammatory response. In CF, these immune cells have been shown to display defective phagocytosis and antimicrobial activity against relevant lung pathogens including *Staphylococcus aureus*, *Pseudomonas aeruginosa* and *Burkholderia cenocepacia* (14–19). *In vitro* and *ex vivo* studies showed some improvement of CF macrophage function following treatment with mono (ivacaftor) or dual (ivacaftor/lumacaftor) correctors (20, 21) as well as a rapid modulation of the transcriptional activity of genes related to inflammation and immune response in peripheral blood cells (22, 23). However, very little is known about the effect of the triple therapy, which is the most efficient from a clinical point of view, on the function of phagocytic cells. Very recently, the recovery of CFTR expression and correction of ATP/P2X7RP signaling, with a consequential reduction of inflammasome activation and circulating pro-inflammatory markers, was shown in monocytes isolated from PWCF under ETI therapy (24).

Here we investigated the impact of ETI therapy on the ability of monocytes to phagocytose bacteria and to kill them when internalized. Additionally, we analyzed the extent to which ETI contributes to the fine balance of the oxidative burst, which has recently been shown as the leading microbicidal mechanism of human macrophages (25).

Methods

PBMCs infection with *P. aeruginosa*, phagocytosis, killing activity and ROS measurements, were performed according to Cavinato et al., 2020 (26). Western blotting and IL-6 quantification were carried out as previously reported (27, 28). Detailed description of materials and methods is reported in supplementary information.

Study subjects

The PWCF (n=41) examined in this study attended the Cystic Fibrosis Regional Center, Regione Lazio. At the time of the study, Trikafta® (Vertex™) was yet to be commercialized. Therefore, PWCF were admitted to the compassionate use of Trikafta® based on their clinical conditions. The study was entirely conducted during the regular care of PWCF , including the collection of blood samples obtained for routine evaluations. Informed written consent was obtained from all of the participants before the start of Trikafta®. All of the methods were carried out in accordance with the relevant guidelines and regulations. Buffy coats, which were not usable for other purposes, were used to isolate cells from healthy donors.

Statistics

All statistical test results were discussed with a biostatistician and performed with GraphPad Prism software. Tests for normality distribution of data were performed, then parametric or non-parametric tests were selected. Details are reported in the figure legends. Differences were significant for a p-value cut-off of 0.05.

Results

ETI therapy rapidly improves the clinical characteristics of PWCF

The clinical efficacy of ETI in real life was evaluated in homozygous (*F508del/F508del*) and heterozygous (*F508del /other*) Caucasian PWCF (Table1), the latter with the second minimal function mutation, as defined in Zemanick *et al.* (2021) (13). At baseline, no difference in the ppFEV1, sweat chloride concentration (SSC), body mass index (BMI) and quality of life (QoL) between the two groups was observed (Table 1). After 1 (M1) and 6 (M6) months from the start of therapy, ppFEV1 significantly increased, while SSC decreased (figure 1). In

particular, the average increase of ppFEV$_1$ in homozygotes was +8.43 ($\pm$ 6.65) in M1 with a further +4.77 ($\pm$ 3.32) in M6, while in heterozygotes, it was +11.81 ($\pm$ 11.61) in M1 with a further + 4.89 ($\pm$ 6.84) in M6. A similar trend was observed in the SSC decrease with a stronger average effect in M1 (-46.29 $\pm$ 26.37 and -44,37 $\pm$ 25.25 in homozygotes and heterozygotes, respectively), compared to M6 (-7.21 $\pm$ 11.87 and $-$ 3.81 $\pm$ 10.81). These results, which were similar to previous clinical trials studies (29, 30) and in more recent studies in real life settings (11–13) highlight the rapid improvement of lung function and CFTR channel activity after ETI therapy. Importantly, this improvement is maintained with a slower increase in the subsequent 5 months. In agreement with ppFEV1 and SSC data, body mass index (BMI) and quality of life (QoL) both improved in the study groups (figure S1). In these measurements no significant differences were observed between homozygotes and heterozygotes PWCF. Collectively, the clinical data showed that all the subjects included in this study responded positively to ETI.

Lung microbiology (Table 1) showed *P. aeruginosa* infection in 37 out of 41 (90.2%) PWCF before therapy. After ETI, 5 PWCF, 4 at M1 and 1 at M6, tested negative for *P. aeruginosa* resulting in an overall reduction of *P. aeruginosa* infection of 13.5%. Multi-species infections, although very limited, were also positively affected by ETI. In particular, *B. cenocepacia* was not detected in two PWCF with *P. aeruginosa* + *B. cenocepacia*, while one patient with *P. aeruginosa* + *S. aureus* resulted negative for *P. aruginosa* (Table 1). Collectively, it appeared that ETI, by improving lung function, also contributed to reducing lung infection.

ETI rapidly improves phagocytosis and the killing activity of *P. aeruginosa* by CF monocytes.

To determine the impact of ETI on the activity of CF monocytes, *P. aeruginosa* phagocytosis and killing before and after therapy were evaluated. Phagocytosis was assessed by determining the number of intracellular viable bacteria recovered from peripheral blood mononuclear cells (PBMCs) infected by *P. aeruginosa*. PBMCs freshly isolated from blood samples, were infected with the PAO1 strain of *P. aeruginosa* expressing GFP (PAO1-GFP) and, after the removal of the non-phagocytosed bacteria by antibiotic treatment, the engulfed bacteria were enumerated by CFU. PBMCs isolated from buffy coats of healthy donors (HD) were included as controls. As reported in figure 2a, at baseline, the CFU recovered from CF cells were significantly lower than those recovered from HD, but the CFU recovered from ETI samples increased significantly. In particular, the average increase of intracellular bacteria compared to the baseline was two-fold at M1 and 2.5-fold at M6 (figure 2a). The uptake of *P. aeruginosa* by monocytes of PWCF was further evaluated by flow cytometry after infection of PBMCs with PAO1-GFP and identification of monocytes by forward and side scatter (figure S2 and figure 2b). Before ETI, the mean percentage of GFP+ monocytes was 1,66-fold lower in PWCF than in HD (figure 2c). After 1 month of ETI treatment, GFP+ monocytes increased significantly, while no significant difference was observed at M6 compared to M1 (figure 2c). In particular with the respect to pre, increased phagocytosis of *P. aeruginosa* was detected in 10 out of 14 PWCF at M1 and in 12 out of 17 at M6 (Table S3). In these analyses, no differences between F508del homozygous and heterozygous CF samples were detected. Control experiments performed in the presence of cytochalasin D, an inhibitor of phagocytosis, failed to reveal GFP+ monocytes confirming the specificity of the assay (figure S3). Moreover, the lack of GFP+ cells in blood lymphocytes, identified by forward and side scatter, confirmed that *P. aeruginosa* uptake was mainly mediated by monocytes (figure S2b).

Collectively, these results demonstrate that 1 month of ETI therapy significantly improves the phagocytic capacity of CF monocytes against *P. aeruginosa,* thus contributing to recovering the phagocytosis defect of these cells, although partially. The improvement gained at M1 was maintained at least for six months in 8 of 10 PWCF, although 5 of them experienced a slight reduction of phagocytosis at the later time point (Table S3). Among the remaining PWCF, 3 showed a further increase of phagocytosis.

Subsequently, the impact of ETI on the bactericidal activity of CF monocytes was assessed. This was done by monitoring the survival of intracellular bacteria 60 min (t60) after the end of infection (t0). Based on the identification of monocytes as the major phagocytic component in PBMCs (figure S2) and in agreement with previously published data (31–33), these cells were used to perform this analysis. As expected, the CFUs recovered from HD cells at t60 were significantly lower than those recovered at t0, with an average decrease in viable bacteria of 56.5%, confirming effective killing of the bacteria (figure 3a and b). At variance, the number of bacteria recovered from CF cells–before ETI did not decrease, rather a very small, but significant, increase was observed (figure 3a). However, one and six months after ETI therapy the CFU recovered 60 min after infection decreased significantly compared to those recovered at the end of infection (figure 3a). Accordingly, the slope of the killing curves of CF PBMCs changed from an average +2,3 before ETI to -24,8 and -17,9 at M1 and M6, respectively (figure 3a). The killing activity, defined as the percentage decrease in CFU, was almost absent in CF cells before therapy (-11.77 %), but increased to 32.5% and 24.3% at M1 and M6, respectively (figure 3b and c). In particular, the improvement of bactericidal activity was observed in all PWCF at M1 and in 8 out of 11 at M6 (Table S4). Notably, although ETI therapy clearly improved both the phagocytic and microbicidal deficiencies, CF PBMCs did not recover completely as they still appeared less active against *P. aeruginosa* compared to non-CF cells, at least in the conditions here examined.

To account for possible differences due to the infecting strain, we compared the microbicidal activity of PBMCs infected with clinical or reference *P. aeruginosa* strains. Taking into consideration that *P. aeruginosa* undergoes continuous adaptation to the CF lung environment, for this analysis we have selected the clonal strains AA2 and AA44, representative of early and late CF isolates, respectively (34). As shown in figure 4, CF PBMCs prior to therapy showed no difference in the ability to kill clinical isolates or PAO1. This result demonstrates that CF PBMCs are similarly deficient against clinical isolates, which support a possible positive effect of ETI on their antimicrobial activity against the clinical *P. aeruginosa* strains.

ETI corrects the exuberant oxidative burst of CF monocytes

It has been recently shown that the optimal bactericidal activity by macrophages against *P. aeruginosa* requires a fine balance between the oxidative and the non-oxidative mechanisms and that excessive and sustained oxidative burst compromises the killing of engulfed bacteria (25). These findings led us to hypothesize a dysregulation of the oxidative burst in CF monocytes as the cause of their defective bactericidal activity. To test this hypothesis, the oxidative burst generated by PAO1-infected PBMCs was determined by measuring the production of the superoxide anion O_2^- with the luminol probe. In infected cells, the probe revealed a rapid increase of O_2^- production followed by a decrease to basal level in about 120 min, while no signal was detected in cells pre-treated with the NADPH oxidase inhibitor DPI, confirming the specificity of the assay (figure S4). Additionally, we identified the monocytes as the major ROS producers in the PBMCs population (figure S5). Quantitative analysis of the chemiluminescence signals showed that the oxidative burst of CF cells before ETI was significantly higher than that of HD controls, but it was significantly reduced at M1 (figure

5a). The higher level of ROS produced by CF cells compared to the controls was further confirmed by the H2DFCDA probe (figure S6).

Next, we evaluated the contribution of the oxidative mechanism to the microbicidal activity of monocytes. For this, bacterial survival was determined in NOX2-inhibited cells, by DPI treatment, and compared to untreated cells. As expected, blocking O_2^- production caused an increase in the recovered CFUs in both non-CF and CF cells (figure 5b, i). However, the increase was higher in HD PBMCs (4.43-fold) than in CF cells (1.6-fold) and it improved after therapy (figure 5b, ii-iii).

These results strongly suggest that microbicidal deficiency of CF monocytes may be due, at least in part, to excessive oxidative burst. This hypothesis was further corroborated by evaluating the activation of NAPDH oxidase at protein level. For this, the $p47^{phox}$ subunit and its phosphorylated form, phospo-$p47^{phox}$ (P-$p47^{phox}$), which accounts for NOX2 activation, were analyzed in monocyte protein lysates. $p47^{phox}$ was higher in CF monocytes before ETI compared to HD monocytes and significantly reduced by 1 month of ETI therapy (figure 6a and b). As expected, $p47^{phox}$ was similar in uninfected and infected monocytes in both non-CF and CF cells (figure 6a and b). Differently, P-$p47^{phox}$ at baseline, although higher in CF respect to HD monocytes, did not change after ETI therapy (figure 6c). However, following infection higher level of P-$p47^{phox}$ was detected in CF monocytes compared to non-CF cells, which was lowered by ETI (figure 6 c). At variance, analysis of $p40^{phox}$ and P-$p40^{phox}$ failed to reveal significant differences between CF and non-CF monocytes (figure S7). In summary, ETI partially reversed this imbalance as $p47^{phox}$ decreased in CF monocytes, while a significant decrease of P-$p47^{phox}$ was limited to infected cells.

Collectively, these results show a clear link between the recovered bactericidal activity and the reduced oxidative burst in monocytes from PWCF under ETI therapy suggesting that ETI

improves the bactericidal activity of monocytes by reducing the excessive oxidative burst of these cells.

ETI reduces the production of IL-6 by CF monocytes

Based on the findings reported above, we wondered whether ETI could also impact the inflammatory response of phagocytic cells. To address this issue, PBMCs, before and after therapy, were challenged with LPS from *P. aeruginosa*, and the pro-inflammatory cytokine IL-6, whose production was reported to be dysregulated in CF innate immune cells, was determined in culture supernatants (28). First, we confirmed that monocytes contributed mainly to the IL-6 produced by PBMCs (figure S8). Next, while similar levels of IL-6 were observed in non-stimulated CF cells, one month after ETI LPS-treated cells showed reduced levels of IL-6, although differences did not reach statistical significance (Figure 7). No difference was observed between homozygote and heterozygote subjects (figure S9).

Discussion

A recent evaluation of the clinical trials with CFTR modulators has confirmed the superior efficacy of the Elexcaftor-Tezacaftor-Ivacaftor triple therapy, compared to the previously developed mono and dual therapy (10). Accordingly, the study group herein analyzed in real life setting and consisting of subjects in urgent need of therapy, responded positively to the therapy as demonstrated by a significant improvement of CF clinical parameters including ppFEV1, SSC, BMI and QoL. Thus, the clinical benefit of ETI supports the validity of the cellular models selected, freshly isolated PBMCs and purified monocytes, to study the impact of ETI on the function of phagocytic cells, whose activity is very relevant for lung homeostasis and defense against invading pathogens. Having confirmed that monocytes are the major phagocytic cells and cytokine producers in the PBMCs populations, they were used

for most of the tests reported here, while pure monocyte were used for protein level analysis. Previous data showed that monocytes from PWCF are impaired in their phagocytic and microbicidal activity compared to healthy controls (31, 32). Here we report that ETI significantly improved both activities, with the highest effect being observed after one month of therapy and the subsequent maintenance of effect over time, up to month 6. Although we could not assess the ETI effect on CF cells infected with clinical *P. aeruginosa* isolates, which is a limit of our study, having observed similar microbicidal defects against PAO1 or clinical strains, it is reasonable to assume that ETI might also improve monocyte-mediated clearance of the clinical isolates. This is also supported by a previous study showing that ivacaftor improves the activity of *in vitro* differentiated CF macrophages infected with a *P. aeruginosa* strain isolated from CF sputum (21).

Collectively, although both phagocytosis and killing of *P. aeruginosa* by CF monocytes did not fully recover in ETI-treated subjects, the observed improvement of their activity might have contributed to the overall recovery of CF disease. This is also supported by lung microbiology which showed a decrease of PWCF positive to *P. aeruginosa* and *B. cenocepacia*.

In order to investigate the molecular mechanism underlying the improved activity of CF monocytes after ETI therapy, we focused our attention on the oxidative burst which has recently been proposed to be the *conditio sine qua non* for the subsequent activation of non-oxidative microbicidal mechanisms (25). Starting from the observation of an exuberant oxidative burst in CF compared to non-CF cells, ETI samples showed a significant reduction of this response down to the similar level of a non-CF cells, which in turn appears to impact positively the microbicidal activity of CF monocytes. Accordingly, the microbicidal activity of the high-ROS producing PBMCs (CF pre) was significantly lower than that of low-ROS producing PBMCs (CF M1 and M6). This is in agreement with very recent investigations, at

single cell level, showing that exaggerated ROS production by macrophages inhibits the overall bactericidal activity (25). This inverse relationship between ROS production and killing efficiency is also confirmed by healthy controls, which displayed low ROS levels and high killing activity when compared to CF cells before ETI.

An exuberant oxidative burst by CF monocytes, compared to healthy cells, was also reported in response to *Aspergillus fumigatus*, which correlated to a worsening of disease severity as assessed by exacerbations and lung functions (33). Conversely, a more disparate effect of dysfunctional CFTR on the oxidative burst of macrophages has been reported. Although ROS produced by monocyte-derived macrophages (MDM), in response to *P. aeruginosa* infection, did not differ between CF and healthy controls, higher ROS production was observed in CF alveolar macrophages compared to CF MDM (16). A further variation was observed in *B. cenocepacia*-infected CF MDM, which produced lower levels of ROS compared to healthy cells, a defect that was assigned to defective activation of NADPH (17). Collectively these results suggest that the oxidative burst response by monocytes and macrophages could be affected differently by the absence of a functional CFTR and by the infecting pathogen.

Based on the current view of the existence of a strict link between oxidative and non-oxidative microbicidal mechanisms which must be finely tuned for the optimal killing of invading pathogens (25) our results strongly suggest that ETI, by reducing the NOX2 NADPH oxidase, improves the overall bactericidal activity of monocytes. This improvement might be due to a more general effect of ETI on protein trafficking to membrane, which in turn contributes to normalizing the assembly and activity of NADPH oxidase and/or as an indirect effect mediated by the rescued CFTR. In particular, it appears that this applies to p47^{phox}, which is consistently elevated in CF monocytes and reduced by ETI, irrespective of *P. aeruginosa* infection. Conversely, NOX2 activation as detected by P-p47^{phox} (35), which appeared highly variable in CF cells thus requiring further investigation, was reduced by ETI

only in infected cells. Other NOX2 subunits, such as p40^{phox}, does not appear to be affected by CFTR dysfunction in monocytes, which is in agreement with a recent demonstration of its irrelevance for NOX2 activity in these cells (36). The possibility that CFTR correctors, by improving CFTR trafficking to membrane, contribute to rescuing other proteins, whose trafficking and activity is linked to CFTR, has been well demonstrated by the recovery of the membrane bound PTEN, in CF monocytes treated with mutation specific CFTR correctors (32). More recently, the effect of the CFTR corrector was also demonstrated in the recovery of ATP-induced P2X7R-mediated inflammasome activation in monocytes, isolated from PWCF undergoing ETI therapy (24). Additionally, it might be speculated that CFTR correctors, by decreasing the respiratory signs and symptoms, might contribute to normalizing the lung microenvironment, thus interfering with the epigenetic reprogramming of immune cells (37).

CF lungs are dominated by high levels of proinflammatory cytokines, which significantly drop after transplantation suggesting that CFTR expression and function are required to control inflammation in the lung environment (38). At present, the recovery of the hyper-inflammatory responses of CF monocytes by ETI treatment has been documented for LPS/ATP induced IL-1β secretion (24). Our data, which show a reduction, although not significant, of the LPS-induced IL-6 secretion by monocytes after ETI therapy, support a broader anti-inflammatory property of ETI therapy whose characterization needs further investigations (24). This and the previous published works, allow us to hypothesize that the molecular pathways, recognized as responsible for specific dysfunctions of CF cells, such as the exuberant inflammatory response or defective microbicidal activity, can be considered for the development of new therapeutic strategies aimed at improving the CF disease. This opportunity appears to be particularly important for the treatment of PWCF who are

unresponsive to CFTR correctors and who may benefit from surrogate therapies that improve host defense against invading pathogens and the management of the inflammatory response.

Table 1. Characteristics of PWCF at initiation of ETI therapy

	F508del/F508del		F508del/other	
Patients (n)	14		27	
Caucasian	14		27	
Sex, Female	7 (50%)		18 (66.6%)	
Age, year	31.43 (±15.81)		28.89 (±14.47)	
pp FEV1	41.66 (±10.34)		51.37 (±14.92)	
SSC (mmol/L)	89 (±15.24)		94.43 (±13.29)	
BMI (Kg/m^2)	19.43 (±3.39)		18.74 (±2.29)	
Lung Microbiology				
	pre	M1/M6	pre	M1/M6
P. aeruginosa	12 (85,7%)	-1/+1	25 (92,6%)	-3/-1
P. aeruginosa + B. cepacia	1 (7,1%)	nc/-1*	1 (3,7%)	nc/-1*
P. aeruginosa + S. aureus	1 (7,1%)	-1/0**		
S. aureus		+1/nc	1 (3,7%)	nc/nc

Data are reported as number, %, or mean ± standard deviation. Abbreviations: ppFEV$_1$, percent-predicted FEV$_1$; SSC, sweat chloride concentration; BMI, body mass index; *P. aeruginosa, Pseudomonas aeruginosa; B. cepacia, Burkholderia cepacia; S. aureus, Staphylococcus aureus;* nc, not changed. Lung Microbiology, number of PWCF with the indicated pathogen. * Negative for *B. cepacia* at M6, *P. aeruginosa* still present; ** negative for *P. aeruginosa* at M1, *S. aureus* still present.

References

1. Elborn JS. Cystic fibrosis. *The Lancet* 2016;388:2519–2531.

2. Mall MA, Mayer-Hamblett N, Rowe SM. Cystic Fibrosis: Emergence of Highly Effective Targeted Therapeutics and Potential Clinical Implications. *Am J Respir Crit Care Med* 2020;201:1193–1208.

3. Amaral MD. How to determine the mechanism of action of CFTR modulator compounds: A gateway to theranostics. *European Journal of Medicinal Chemistry* 2021;210:112989.

4. Kleizen B, Hunt JF, Callebaut I, Hwang T-C, Sermet-Gaudelus I, Hafkemeyer S, Sheppard DN. CFTR: New insights into structure and function and implications for modulation by small molecules. *Journal of Cystic Fibrosis* 2020;19:S19–S24.

5. Van Goor F, Yu H, Burton B, Hoffman BJ. Effect of ivacaftor on CFTR forms with missense mutations associated with defects in protein processing or function. *J Cyst Fibros* 2014;13:29–36.

6. Ramsey BW, Davies J, McElvaney NG, Tullis E, Bell SC, Dřevínek P, Griese M, McKone EF, Wainwright CE, Konstan MW, Moss R, Ratjen F, Sermet-Gaudelus I, Rowe SM, Dong Q, Rodriguez S, Yen K, Ordoñez C, Elborn JS, VX08-770-102 Study Group. A CFTR potentiator in patients with cystic fibrosis and the G551D mutation. *N Engl J Med* 2011;365:1663–1672.

7. Taylor-Cousar JL, Munck A, McKone EF, van der Ent CK, Moeller A, Simard C, Wang LT, Ingenito EP, McKee C, Lu Y, Lekstrom-Himes J, Elborn JS. Tezacaftor–Ivacaftor in Patients with Cystic Fibrosis Homozygous for Phe508del. *N Engl J Med* 2017;377:2013–2023.

8. Taylor-Cousar JL, Mall MA, Ramsey BW, McKone EF, Tullis E, Marigowda G, McKee CM, Waltz D, Moskowitz SM, Savage J, Xuan F, Rowe SM. Clinical development of triple-combination CFTR modulators for cystic fibrosis patients with one or two *F508del* alleles. *ERJ Open Res* 2019;5:00082–02019.

9. Wainwright CE, Elborn JS, Ramsey BW, Marigowda G, Huang X, Cipolli M, Colombo C, Davies JC, De Boeck K, Flume PA, Konstan MW, McColley SA, McCoy K, McKone EF, Munck A, Ratjen F, Rowe SM, Waltz D, Boyle MP, TRAFFIC Study Group,

TRANSPORT Study Group. Lumacaftor-Ivacaftor in Patients with Cystic Fibrosis Homozygous for Phe508del CFTR. *N Engl J Med* 2015;373:220–231.

10. Southern KW, Murphy J, Sinha IP, Nevitt SJ. Corrector therapies (with or without potentiators) for people with cystic fibrosis with class II CFTR gene variants (most commonly F508del). *Cochrane Database Syst Rev* 2020;CD010966.doi:10.1002/14651858.CD010966.pub3.

11. Nichols DP, Paynter AC, Heltshe SL, Donaldson SH, Frederick CA, Freedman SD, Gelfond D, Hoffman LR, Kelly A, Narkewicz MR, Pittman JE, Ratjen F, Rosenfeld M, Sagel SD, Schwarzenberg SJ, Singh PK, Solomon GM, Stalvey MS, Clancy JP, Kirby S, Van Dalfsen JM, Kloster MH, Rowe SM. Clinical Effectiveness of Elexacaftor/Tezacftor/Ivacaftor in People with Cystic Fibrosis. *Am J Respir Crit Care Med* 2021;doi:10.1164/rccm.202108-1986OC.

12. Burgel P-R, Durieu I, Chiron R, Ramel S, Danner-Boucher I, Prevotat A, Grenet D, Marguet C, Reynaud-Gaubert M, Macey J, Mely L, Fanton A, Quetant S, Lemonnier L, Paillasseur J-L, Da Silva J, Martin C, Andrejak C, Becourt A, Mounard J, Poulet C, Rames C, Talleux M, Chevalier M-C, Darviot E, Jouvenot M, Marien C, Paris A, Pelatan C, *et al.* Rapid Improvement after Starting Elexacaftor–Tezacaftor–Ivacaftor in Patients with Cystic Fibrosis and Advanced Pulmonary Disease. *Am J Respir Crit Care Med* 2021;204:64–73.

13. Zemanick ET, Taylor-Cousar JL, Davies J, Gibson RL, Mall MA, McKone EF, McNally P, Ramsey BW, Rayment JH, Rowe SM, Tullis E, Ahluwalia N, Chu C, Ho T, Moskowitz SM, Noel S, Tian S, Waltz D, Weinstock TG, Xuan F, Wainwright CE, McColley SA. A Phase 3 Open-Label Study of Elexacaftor/Tezacaftor/Ivacaftor in Children 6 through 11 Years of Age with Cystic Fibrosis and at Least One F508del Allele. *Am J Respir Crit Care Med* 2021;203:1522–1532.

14. Di A, Brown ME, Deriy LV, Li C, Szeto FL, Chen Y, Huang P, Tong J, Naren AP, Bindokas V, Palfrey HC, Nelson DJ. CFTR regulates phagosome acidification in macrophages and alters bactericidal activity. *Nat Cell Biol* 2006;8:933–944.

15. Del Porto P, Cifani N, Guarnieri S, Di Domenico EG, Mariggiò MA, Spadaro F, Guglietta S, Anile M, Venuta F, Quattrucci S, Ascenzioni F. Dysfunctional CFTR alters the bactericidal activity of human macrophages against Pseudomonas aeruginosa. *PLoS ONE* 2011;6:e19970.

16. Cifani N, Pompili B, Anile M, Patella M, Diso D, Venuta F, Cimino G, Quattrucci S, Di Domenico EG, Ascenzioni F, Porto PD. Reactive-Oxygen-Species-Mediated P. aeruginosa Killing Is Functional in Human Cystic Fibrosis Macrophages. *PLoS One* 2013;8:.

17. Assani K, Shrestha CL, Robledo-Avila F, Rajaram MV, Partida-Sanchez S, Schlesinger LS, Kopp BT. Human Cystic Fibrosis Macrophages Have Defective Calcium-Dependent PKC Activation of the NADPH Oxidase, an Effect Augmented by Burkholderia cenocepacia. *J Immunol* 2017;198:1985–1994.

18. Li C, Wu Y, Riehle A, Ma J, Kamler M, Gulbins E, Grassmé H. Staphylococcus aureus Survives in Cystic Fibrosis Macrophages, Forming a Reservoir for Chronic Pneumonia. *Infect Immun* 2017;85:e00883-16.

19. Assani K, Tazi MF, Amer AO, Kopp BT. IFN-γ stimulates autophagy-mediated clearance of Burkholderia cenocepacia in human cystic fibrosis macrophages. *PLoS One* 2014;9:e96681.

20. Barnaby R, Koeppen K, Nymon A, Hampton TH, Berwin B, Ashare A, Stanton BA. Lumacaftor (VX-809) restores the ability of CF macrophages to phagocytose and kill Pseudomonas aeruginosa. *Am J Physiol Lung Cell Mol Physiol* 2018;314:L432–L438.

21. Zhang S, Shrestha CL, Kopp BT. Cystic fibrosis transmembrane conductance regulator (CFTR) modulators have differential effects on cystic fibrosis macrophage function. *Sci Rep* 2018;8:.

22. Hisert KB, Birkland TP, Schoenfelt KQ, Long ME, Grogan B, Carter S, Liles WC, McKone EF, Becker L, Manicone AM, Gharib SA. CFTR Modulator Therapy Enhances Peripheral Blood Monocyte Contributions to Immune Responses in People With Cystic Fibrosis. *Front Pharmacol* 2020;11:1219.

23. Kopp BT, Fitch J, Jaramillo L, Shrestha CL, Robledo-Avila F, Zhang S, Palacios S, Woodley F, Hayes D, Partida-Sanchez S, Ramilo O, White P, Mejias A. Whole-blood transcriptomic responses to lumacaftor/ivacaftor therapy in cystic fibrosis. *J Cyst Fibros* 2020;19:245–254.

24. Gabillard-Lefort C, Casey M, Glasgow AMA, Boland F, Kerr O, Marron E, Lyons A-M, Gunaratnam C, McElvaney NG, Reeves EP. Trikafta Rescues CFTR and Lowers Monocyte P2X7R-Induced Inflammasome Activation in Cystic Fibrosis. *Am J Respir Crit Care Med* 2022;doi:10.1164/rccm.202106-1426OC.

25. Riazanski V, Sui Z, Nelson DJ. Kinetic Separation of Oxidative and Non-oxidative Metabolism in Single Phagosomes from Alveolar Macrophages: Impact on Bacterial Killing. *iScience* 2020;23:101759.

26. Cavinato L, Genise E, Luly FR, Di Domenico EG, Del Porto P, Ascenzioni F. Escaping the Phagocytic Oxidative Burst: The Role of SODB in the Survival of Pseudomonas aeruginosa Within Macrophages. *Front Microbiol* 2020;11:326.

27. Mecocci S, Gevi F, Pietrucci D, Cavinato L, Luly FR, Pascucci L, Petrini S, Ascenzioni F, Zolla L, Chillemi G, Cappelli K. Anti-Inflammatory Potential of Cow, Donkey and Goat Milk Extracellular Vesicles as Revealed by Metabolomic Profile. *Nutrients* 2020;12:.

28. Luly FR, Lévêque M, Licursi V, Cimino G, Martin-Chouly C, Théret N, Negri R, Cavinato L, Ascenzioni F, Del Porto P. MiR-146a is over-expressed and controls IL-6 production in cystic fibrosis macrophages. *Sci Rep* 2019;9:16259.

29. Keating D, Marigowda G, Burr L, Daines C, Mall MA, McKone EF, Ramsey BW, Rowe SM, Sass LA, Tullis E, McKee CM, Moskowitz SM, Robertson S, Savage J, Simard C, Van Goor F, Waltz D, Xuan F, Young T, Taylor-Cousar JL, VX16-445-001 Study Group. VX-445-Tezacaftor-Ivacaftor in Patients with Cystic Fibrosis and One or Two Phe508del Alleles. *N Engl J Med* 2018;379:1612–1620.

30. Middleton PG, Mall MA, Dřevínek P, Lands LC, McKone EF, Polineni D, Ramsey BW, Taylor-Cousar JL, Tullis E, Vermeulen F, Marigowda G, McKee CM, Moskowitz SM, Nair N, Savage J, Simard C, Tian S, Waltz D, Xuan F, Rowe SM, Jain R, VX17-445-102 Study Group. Elexacaftor-Tezacaftor-Ivacaftor for Cystic Fibrosis with a Single Phe508del Allele. *N Engl J Med* 2019;381:1809–1819.

31. Van de Weert-van Leeuwen PB, Van Meegen MA, Speirs JJ, Pals DJ, Rooijakkers SHM, Van der Ent CK, Terheggen-Lagro SWJ, Arets HGM, Beekman JM. Optimal complement-mediated phagocytosis of Pseudomonas aeruginosa by monocytes is cystic fibrosis transmembrane conductance regulator-dependent. *Am J Respir Cell Mol Biol* 2013;49:463–470.

32. Riquelme SA, Hopkins BD, Wolfe AL, DiMango E, Kitur K, Parsons R, Prince A. Cystic Fibrosis Transmembrane Conductance Regulator Attaches Tumor Suppressor PTEN to the Membrane and Promotes Anti Pseudomonas aeruginosa Immunity. *Immunity* 2017;47:1169-1181.e7.

33. Brunel SF, Willment JA, Brown GD, Devereux G, Warris A. Aspergillus-induced superoxide production by cystic fibrosis phagocytes is associated with disease severity. *ERJ Open Res* 2018;4:.

34. Cigana C, Curcurù L, Leone MR, Ieranò T, Lorè NI, Bianconi I, Silipo A, Cozzolino F, Lanzetta R, Molinaro A, Bernardini ML, Bragonzi A. Pseudomonas aeruginosa Exploits Lipid A and Muropeptides Modification as a Strategy to Lower Innate Immunity during Cystic Fibrosis Lung Infection. *PLoS One* 2009;4:e8439.

35. Begum R, Thota S, Abdulkadir A, Kaur G, Bagam P, Batra S. NADPH oxidase family proteins: signaling dynamics to disease management. *Cell Mol Immunol* 2022;19:660–686.

36. van de Geer A, Nieto-Patlán A, Kuhns DB, Tool AT, Arias AA, Bouaziz M, de Boer M, Franco JL, Gazendam RP, van Hamme JL, van Houdt M, van Leeuwen K, Verkuijlen PJ, van den Berg TK, Alzate JF, Arango-Franco CA, Batura V, Bernasconi AR, Boardman B, Booth C, Burns SO, Cabarcas F, Bensussan NC, Charbit-Henrion F, Corveleyn A, Deswarte C, Azcoiti ME, Foell D, Gallin JI, *et al.* Inherited p40phox deficiency differs from classic chronic granulomatous disease. *J Clin Invest* 2018;128:3957–3975.

37. Hey J, Paulsen M, Toth R, Weichenhan D, Butz S, Schatterny J, Liebers R, Lutsik P, Plass C, Mall MA. Epigenetic reprogramming of airway macrophages promotes polarization and inflammation in muco-obstructive lung disease. *Nat Commun* 2021;12:6520.

38. Patella M, Anile M, Del Porto P, Diso D, Pecoraro Y, Onorati I, Mantovani S, De Giacomo T, Ascenzioni F, Rendina EA, Venuta F. Role of cytokine profile in the differential diagnosis between acute lung rejection and pulmonary infections after lung transplantation†. *Eur J Cardiothorac Surg* 2015;47:1031–1036.

Figure 1. Improvement of ppFEV1 and sweat chloride concentration (SSC) after ETI therapy. ppFEV$_1$ (a) and SSC (b) in homozygous (n=14) and heterozygous (n=27) PWCF before (pre) and after 1 (M1) and 6 (M6) months of therapy. Box plots with median and whiskers pointing to min and max values. The one-way ANOVA with Tukey's multiple comparison test was used; *, p<0.05; **, 0.01; ****, p<0.0001.

Figure 2. ETI improves the phagocytic activity of CF monocytes. *P. aeruginosa* uptake by PBMCs isolated from HD and PWCF pre, M1 and M6. a) CFU recovered after the end of infection. Left panel, scattered dot plot with mean ± SEM; the Kruska-Wallis test with Dunn's multiple comparison was used. Right panel, longitudinal analysis of data; the Friedman test with Dunn's multiple comparison was used. b) Representative overlaid histograms of monocytes infected with PAO1-GFP. c) Bacterial uptake (GFP$^+$ monocyte, %). Left panel, scattered dot plot with mean ± SEM; the Brown-Forsythe ANOVA with t-test for multiple comparison was used. Right panel, longitudinal analysis of data; the mixed-effect model (REML) with Tukey's multiple comparison test was used. *, p<0.05; **, 0.01; ***, p<0.001; ****, p<0.0001.

Figure 3. Improvement of microbicidal activity by ETI. a) *P. aeruginosa* survival in PBMCs isolated from HD and PWCF pre, M1 and M6; CFUs recovered at the end of infection (0) and 60 min after infection (60). The average slopes are reported above the 0-60 connecting lines. Slopes were calculated with the linear regression model; the Wilcoxon test was used. b) Killing activity reported as the decrease of CFUs (%) in 60 min after infection; scattered dot plot mean ± SEM; the Kruska-Wallis test with Dunn's multiple comparison was used. c) Longitudinal analysis of data; the Friedman test with Dunn's multiple comparison was used. *, p<0.05; **, 0.01; ***, p<0.001; ****, p<0.0001.

Figure 4. Microbicidal activity of PBMCs against *P. aeruginosa* PAO1 and clinical isolates. a) PBMCs from HD and PWCF before ETI (pre) infected with PAO1. Demographic and clinical characteristics of PWCF are reported in table S3. Student's t-test was used. b) PBMCs from PWCF pre infected with PAO1 or the clinical isolates AA2 and AA44. One-way ANOVA test with Tukey's multiple comparison test was used. Scattered dot plot with mean ± SEM; *, p<0.05.

Figure 5. ETI reduces the exuberant oxidative-burst and improves microbicidal activity. a) O_2^- production by infected PBMCs as detected by the luminol assay. i) Representative kinetics of O_2^- production. ii) quantitative analysis of O_2^- produced by the indicated samples (AUC, area under the curve). Scattered dot plot with mean ± SEM; Kruska-Wallis test with Dunn's multiple comparison was used. iii) Longitudinal analysis of data. The Friedman test with Dunn's multiple comparison was used. b) CFUs recovered from untreated or DPI-treated PBMCs. i) CFUs recovered from PAO1-infected cells. The Wilcoxon test was used. ii) Fold increase of CFUs in DPI treated respect to untreated cells. Scattered dot plot with mean ± SEM; Kruska-Wallis test with Dunn's multiple comparison was used. iii) longitudinal analysis of data; Friedman test with Dunn's multiple comparison was used. *, $p<0.05$; **, 0.01; ***, $p<0.001$.

Figure 6. ETI rapidly reduces the high level of NOX2 activation. Analysis of the p47^{phox} and P-p47^{phox} NOX2 subunits in monocytes from HD (n=6), PWCF pre (n=6) and M1 (n=6). a) Representative blots of cell lysates from non-infected and PAO1-infected monocytes. GAPDH, loading control. b and c) quantitative analysis of p47^{phox} and P-p47^{phox}, respectively. Data are presented as mean ± SEM; Brown-Forsythe ANOVA test with t-test for multiple comparison was used. *, $p<0.05$; **, 0.01; ***, $p<0.001$; ****, $p<0.0001$.

Figure 7. ETI decreases IL-6 production by LPS-treated cells. IL-6 in supernatants of CF pre and M1 PBMCs at baseline (untreated) and after LPS induction. Empty symbols, *F508del* homozygotes; grey symbols, *F508del* heterozygotes. The two-way ANOVA with Bonferroni multiple comparison test was used; **, $p<0.01$; ****, $p<0.0001$.
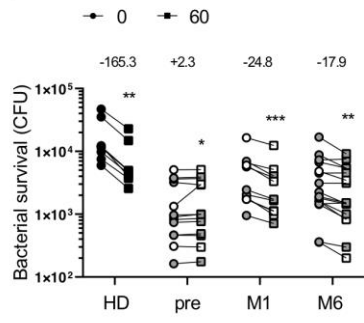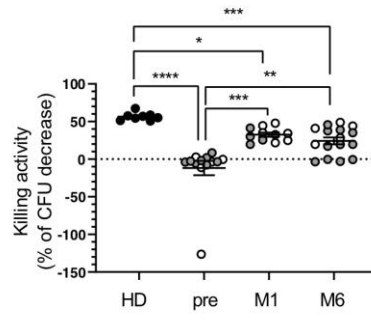
a)

F508del/F508del
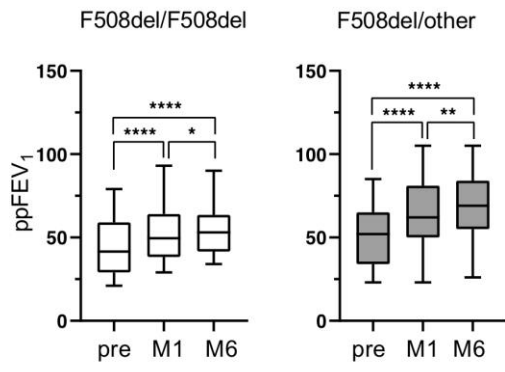
F508del/other

b)
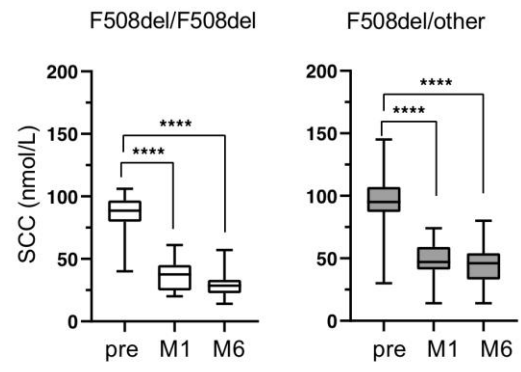
F508del/F508del
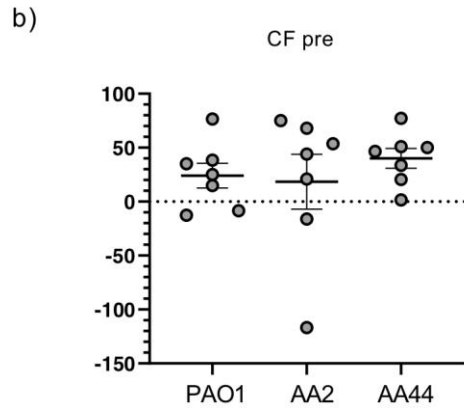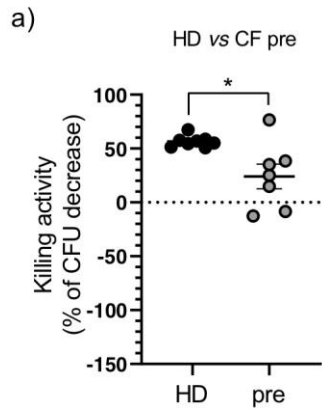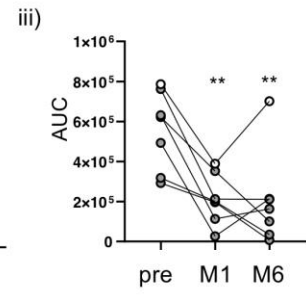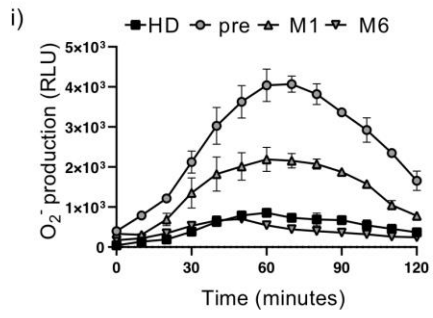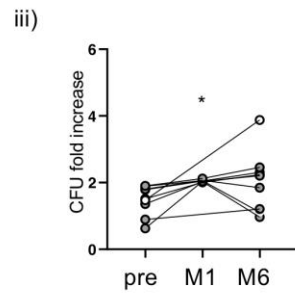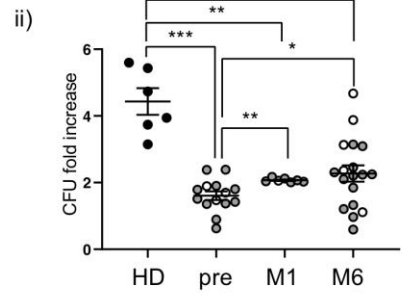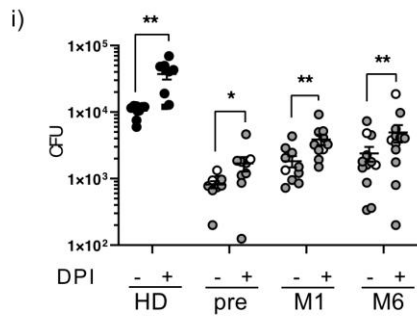
F508del/other

○ F508del/F508del　◉ F508del/other

a)

b)

Uninfected　+ PAO1-GFP

HD　pre　M1　M6

Counts

GFP

c)

a) HD *vs* CF pre

b) CF pre

○ F508del/F508del ◐ F508del/other

a)

i) O₂⁻ production (RLU) vs Time (minutes); HD, pre, M1, M6

ii) AUC: HD, pre, M1, M6 ** ** **

iii) AUC: pre, M1, M6 ** **

b)

i) CFU vs DPI (- +) for HD, pre, M1, M6 ** * ** **

ii) CFU fold increase: HD, pre, M1, M6 *** ** ** * **

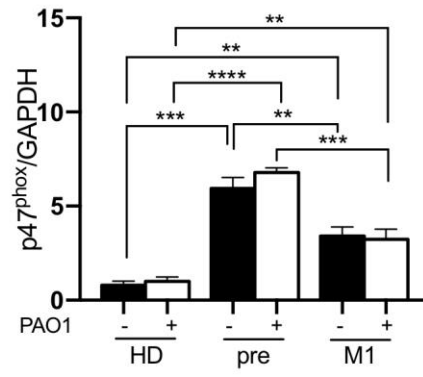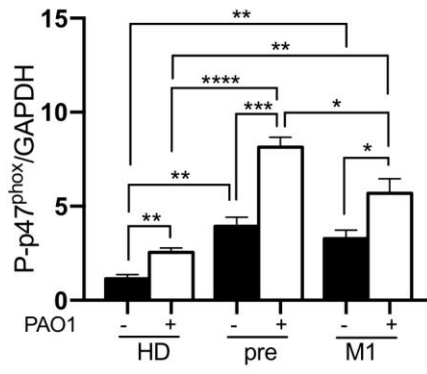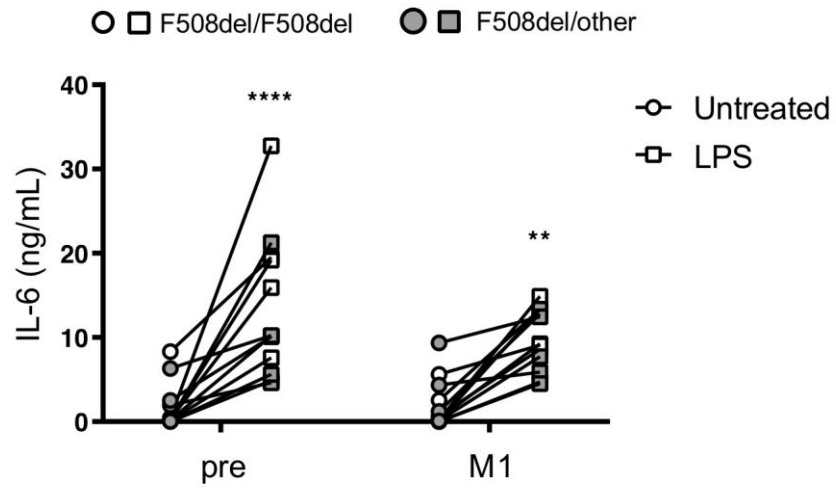iii) CFU fold increase: pre, M1, M6 *
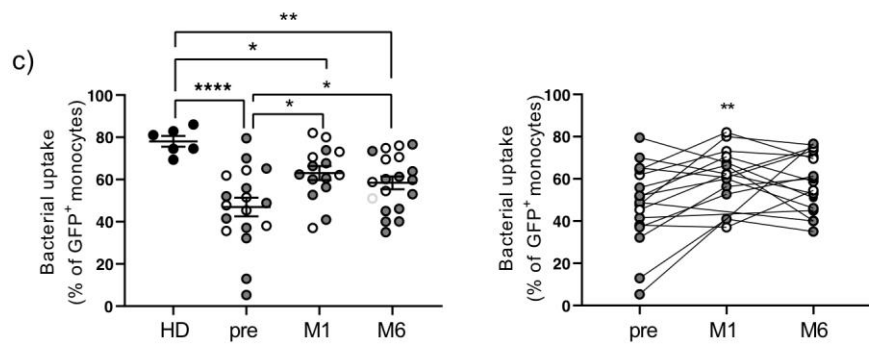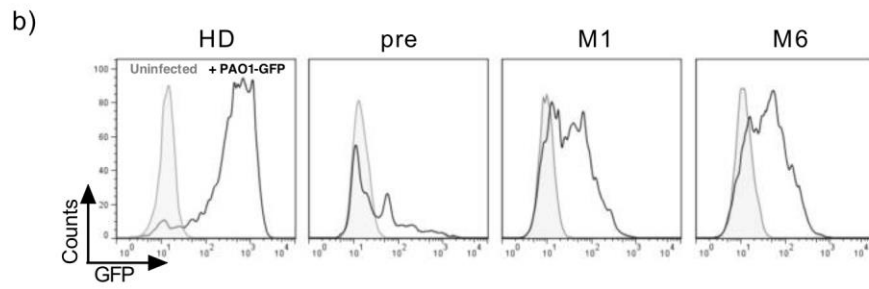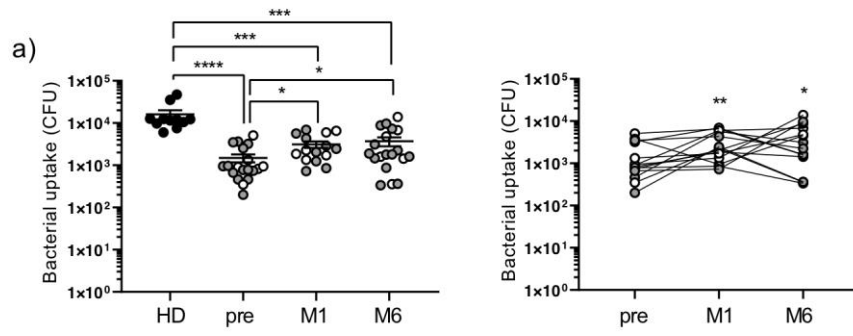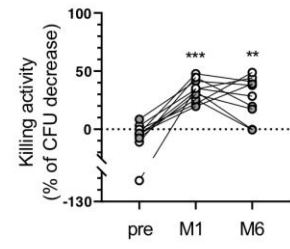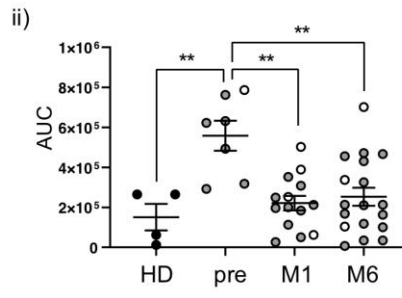
a)
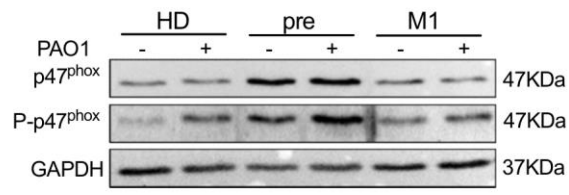
b)

c)

Data Supplement

Abbreviations:
HD, healthy donors
pre, CF patients before therapy
M1, CF patients after 1 month of therapy
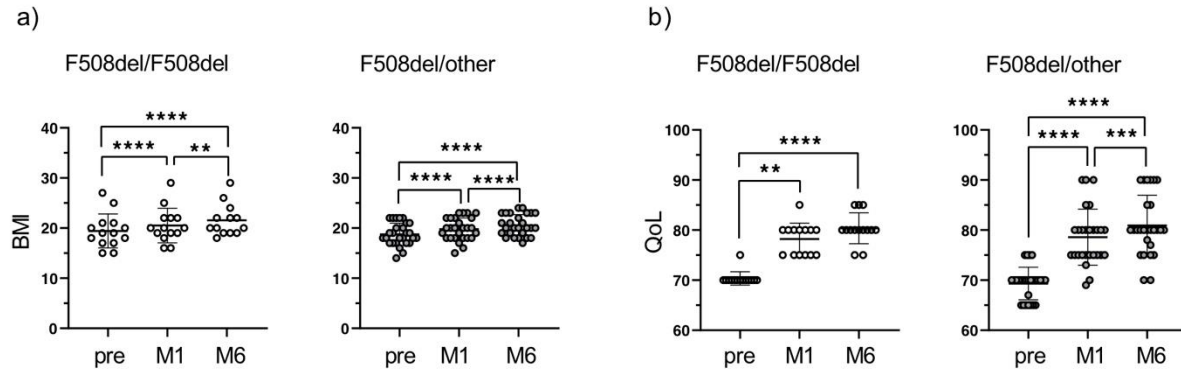M6, CF patients after and 6 months of therapy

Figure S1. Improvement of body mass index (BMI) and quality of life (QoL) in patients treated with ETI. BMI and QoL in CF patients pre, M1 and M6. a) BMI of F508del/F508del (pre and M1, n=14; M6, n=13) and F508del/other (n=27). The mixed effect-model (REML) with Tukey's multiple comparison (left) and the one-way ANOVA with Tukey's multiple comparison (right) were used. b) QoL of F508del/F508del (n=14) and F508del/other (n=27). The one-way ANOVA with Tukey's multiple comparison was used. Scattered dot plot, with mean ± SEM; *, p<0.05; **, 0.01; ***, p<0.001; ****, p<0.0001.
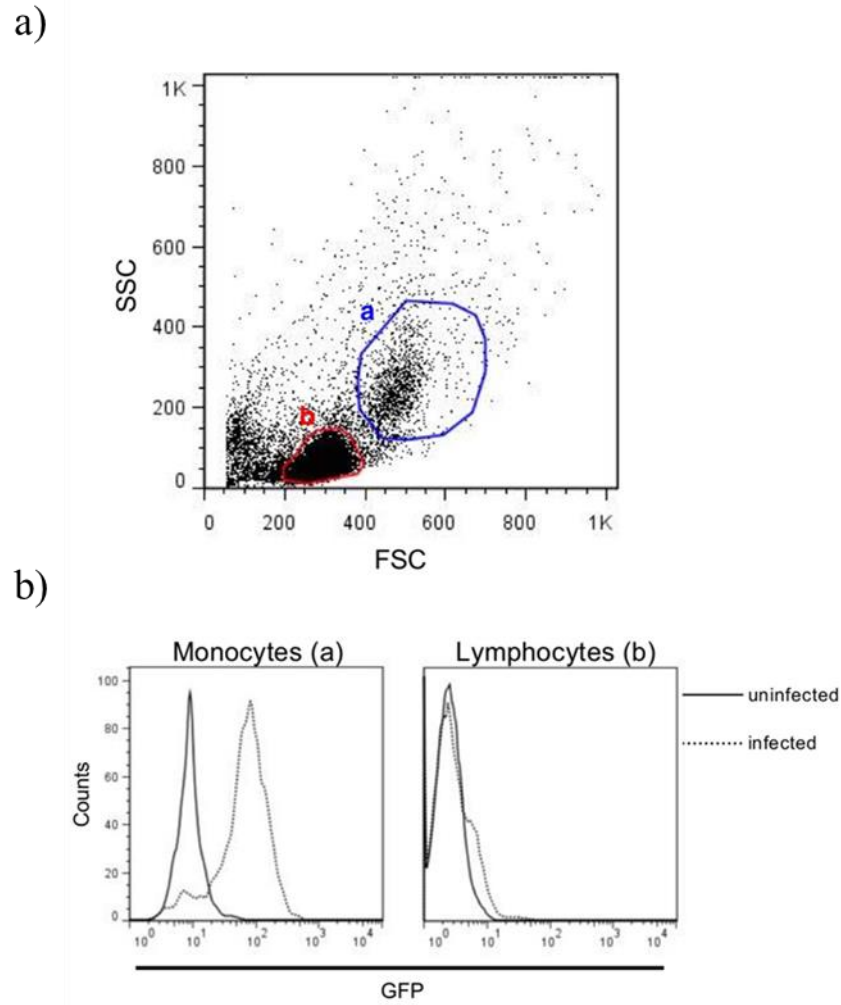
Figure S2. *P. aeruginosa* **is phagocytosed only by monocytes.** HD PBMCs were infected with PAO1-GFP and the phagocytosis was evaluated by flow cytometry. a) Gate strategies to identify PBMCs populations: monocytes (gate a) and lymphocytes (gate b). b) Overlaid histograms of infected monocytes (gate a) and lymphocytes (gate b). Heavy line, uninfected controls; dotted line, infected cells.
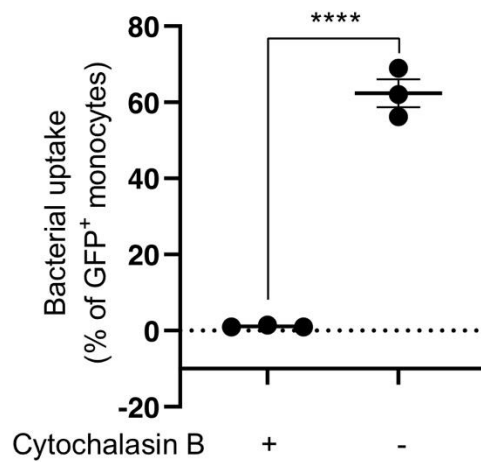
Figure S3. Cytochalasin B treatment inhibits phagocytic activity of monocytes. HD PBMCs, pretreated or not with Cytochalasin B, were infected with PAO1-GFP and phagocytosis was evaluated by flow cytometry. Scattered dot plot with mean ± SEM. Student's t-tests was used; ****, p<0,0001.
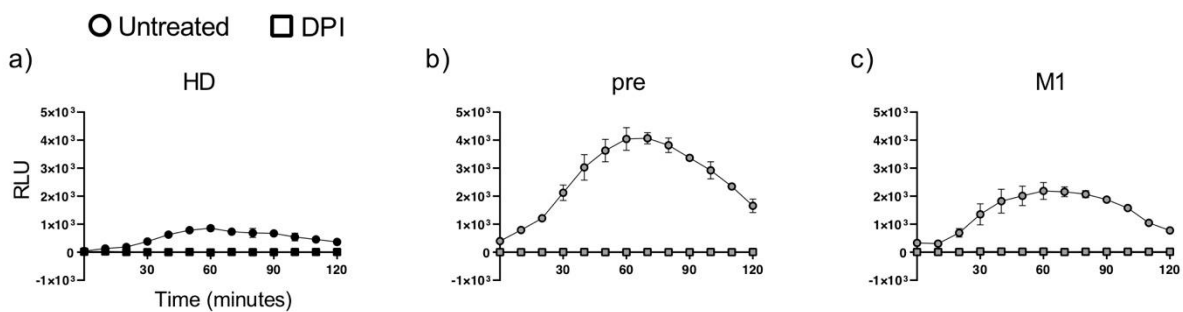

Figure S4. Diphenyleneiodonium (DPI) treatment inhibits NOX2-dependent ROS production. Samples: PBMC from HD (a) and CF pre (b) and M1 (c), pretreated (squares) or not (circles) with DPI. ROS production, following PAO1 infection, was detected every 10 min and reported as relative light unit (RLU). Data are mean ± SD of three technical replicates.
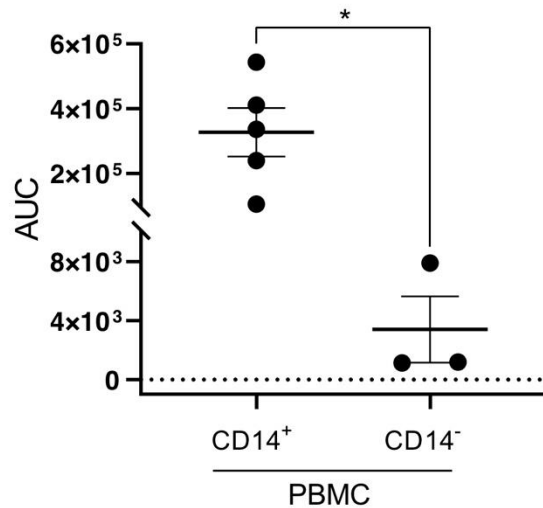
Figure S5. O_2^- production by infected HD PBMC depleted of CD14$^+$ cells. Samples: PAO1-infected PBMC (CD14$^+$) and PAO1-infected PBMC depleted of CD14$^+$ cells (CD14$^-$). O_2^- production was measured every 10 min and quantified from kinetic curves as area under the curve (AUC). The Mann-Whitney test was used. Scattered dot plot with mean ± SEM; *, $p<0.05$.
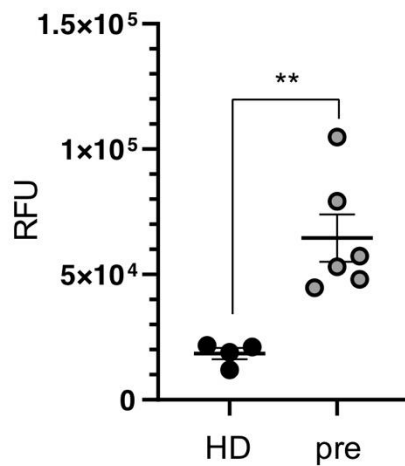
Figure S6. ROS production as detected by the H2DCFDA probe. Samples: PBMCs from HD and CF pre. Cells were infected with PAO1 and the resulting oxidative burst was measured 60 min after infection. Total ROS production is reported as relative fluorescent unit (RFU). The Student's t-test was used. Scattered dot plot with mean ± SEM; **, $p<0.01$.

Figure S7. p40^phox and P-p40^phox in HD and CF monocytes. a) Representative WBs of two HD and two CF pre. b and c) Quantitative analysis of $p40^{phox}$ and $P\text{-}p40^{phox}$ respect to the loading control, GAPDH. The Brown-Forsythe ANOVA test with t-test for multiple comparison was used without detection of statistical significance among samples. Scattered dot plot with mean ± SEM.
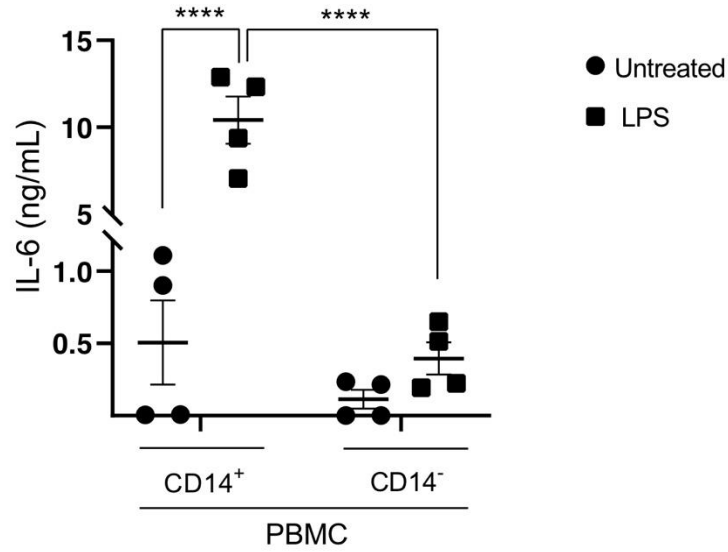
Figure S8. CD14+ cells depletion abolishes IL-6 production by LPS-challenged PBMC. HD PBMC depleted (CD14-) or not depleted (CD14+) remained untre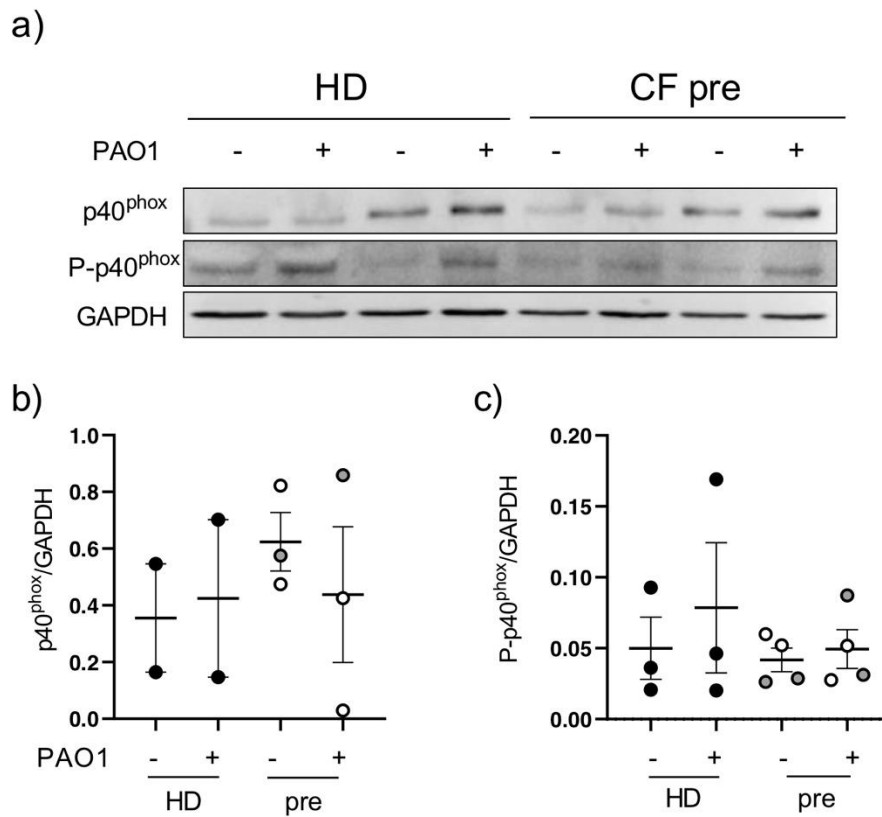ated or were stimulated with LPS. IL-6 secretion in supernatants was measured by ELISA. The two-way ANOVA test with Bonferroni multiple comparison was used. Scatter dot plot with mean ± SEM; ****, $p < 0.0001$.
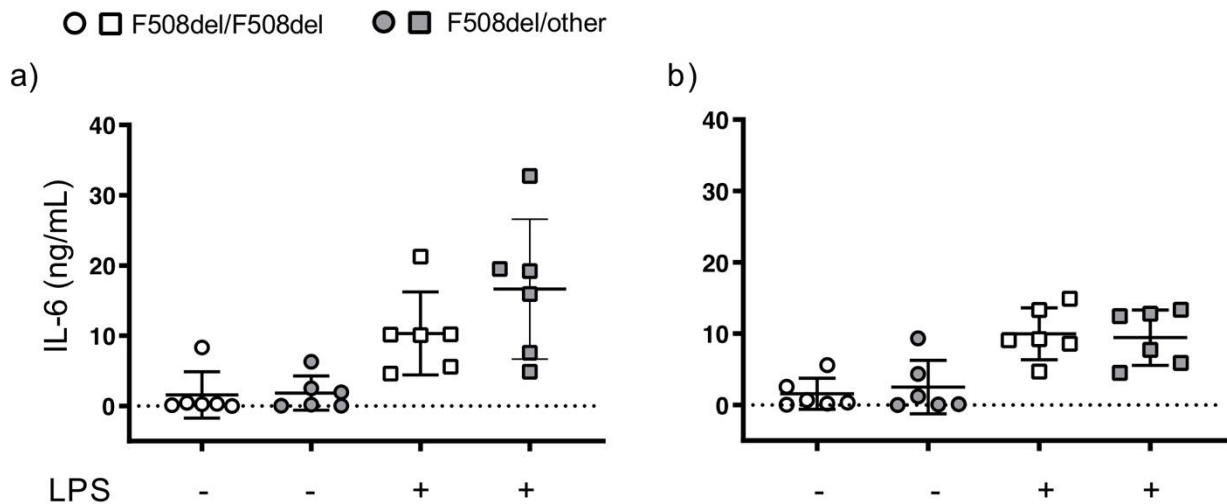
Figure S9. IL-6 production by homozygous and heterozygous patients. IL-6 secretion in supernatants of PBMCs from CF pre (a) and M1 (b). Kruskal-Wallis with Dunn multiple comparison test was used. Differences between homozygous and heterozygous subjects were not significant. Scatter dot plot with mean ± SEM.

Figure S10. All blots examined for the analysis of $p47^{phox}$ and $P\text{-}p47^{phox}$

Figure S11. All blots examined for the analysis of $p40^{phox}$ and $P\text{-}p40^{phox}$

Supplementary materials and methods

Table S1. Reagents, Suppliers and Identification Code (ID)

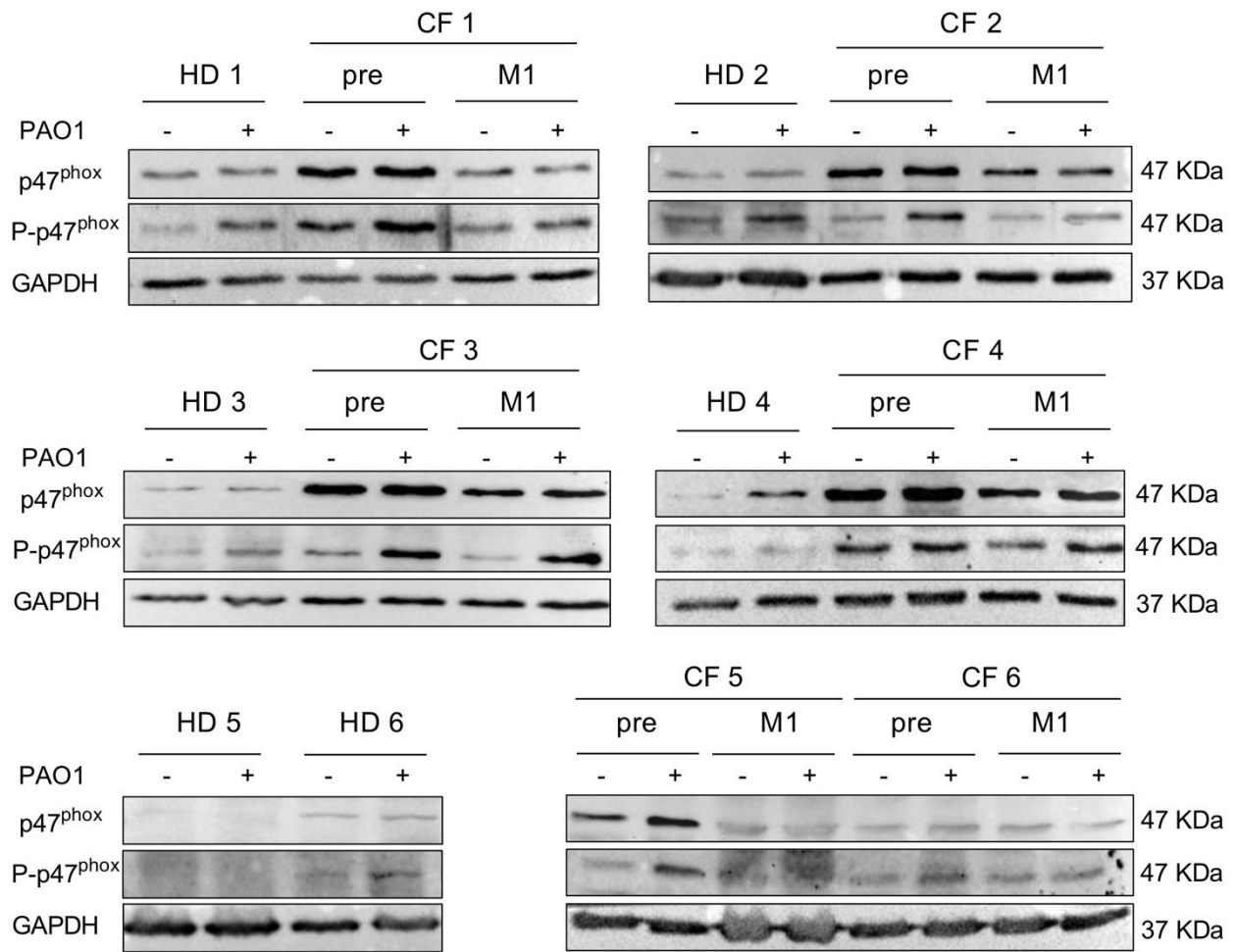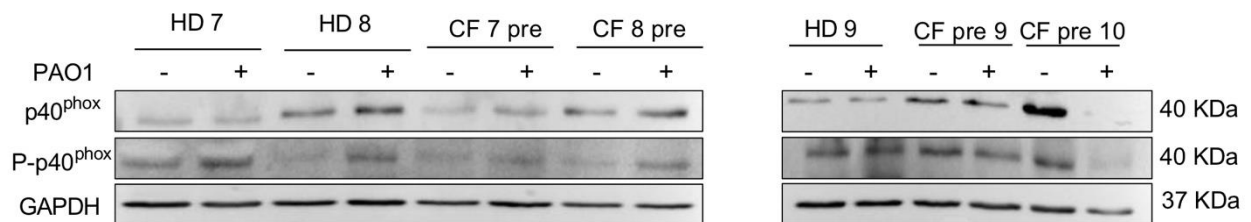| Reagent	Suppliers	ID
Anti-human Phospho-p47^{phox} (ser345) (WB, diluted 1/500)	Invitrogen	PA537806
Anti-human p47^{phox} (WB, diluted 1/500)	Santa Cruz	sc-17845
Anti-human p40^{phox} (WB, diluted 1/500)	Santa Cruz	sc-48388
Anti-human Phospho-p40^{phox} (thr154) (WB, diluted 1/1000)	Cell Signaling	#4311
Anti-GAPDH	Santa Cruz	sc-47724
Anti-human CD14	Immunotools	21620146
Anti-mouse Control IgG	Immunotools	21815016
Anti-mouse IgG	GE Healthcare	NA931V
Anti-rabbit IgG	GE Healthcare	NA934V
EasySep monocyte enrichment kit without CD16 depletion, EasySep^{TM}	StemCell	#19058
CD14 MicroBeads human	Miltenyi	130-050201
IL-6 Elisa kit	R&D	DY008
P. aeruginosa LPS	Sigma	L8643
diphenyleneiodonium (DPI)	Sigma-Aldrich	D2926
Luminol	Sigma-Aldrich	123072
2',7'-dichlorodihydrofluorescein diacetate (H2DCFDA)	Thermo Fisher Scientific	D399
Lympholyte	CEDERLANE	CL5020
RPMI with glutamine	Corning	10-040-CV
Fetal Bovine Serum (FBS)	Euroclone	ECS0180l
Premium FBS (low endotoxin)	Corning	35-015
Penicillin-Streptomycin	Corning	30-002-CI
LB Broth	Sigma	L3022
Agar	Sigma	A1296
Amikacin	Sigma	A1774
Ceftazidime	Sigma	C3809
Gentamycin	Sigma	G3632
HBSS w/o Calcium, Magnesium, Sodium Bicarbonate, Phenol Red	Euroclone	ECM0507L
Dulbecco's Phosphate Buffered Saline (DPBS) w/o Calcium Chloride, Magnesium Chloride	Sigma	D8537
BSA	Sigma	A4503
Tween®20	Sigma	P7949
Nonfat dried milk powder	ITW Reagents	A0830

Table S2. Characteristics of patients with cystic fibrosis at initiation of ETI therapy examined in supplementary figure 4, S6, S7 and S11

	F508del/F508del	*F508del/other*
N of patients	2	7
Sex, Female	2 (100%)	3 (42,8%)
Age, year	24 (±19.8)	31,57 (±13.1)
pp FEV1	70.5 (±12.02)	85.14 (±28.65)
SSC (mmol/L)	82.5 (±4.95)	90.86 (±27.11)
BMI (Kg/m^2)	17.5 (±3.53)	22.86 (±4.18)
QoL	72,5 (±3.53)	77.29 (±10.08)
Lung Microbiology		
P. aeruginosa	1 (50%)	5 (71,4%)
S. aureus		2 (28,5%)

Data are reported as number, %, or mean ± standard deviation. Abbreviations: ppFEV$_1$, percent-predicted FEV$_1$; SSC, sweat chloride concentration; BMI, body mass index. Lung microbiology, the number and the percentage of patients with the indicated pathogen I reported.

Table S3. Percentage of GFP⁺ monocytes in PAO1-GFP infected PBMC from CF pre, M1 and M6

pre	M1	M6
79,5	67,7	51
70	62,35	53,07
65,2	60,6	73,45↑
64,4	**82↑**	**69,54↑**
61,9	**73,15↑**	**70,66↑**
55,9	66,35↑	40,1
52	60↑	46,1
51,58	**70,5↑**	**58,79↑**
48,9	nd	40
47,8	**80↑**	**76↑**
45,4	**62,1↑**	**74,9↑**
41,5	nd	45↑
38	**37**	**54,5↑**
37,14	52,68↑	61,31↑
35,6	nd	nd
32,2	56,4↑	60,2↑
12,94	40,95↑	35,07↑
5,3	nd	76,6↑
nd	nd	63,9
nd	nd	59,75
nd	73,9	nd

Each row refers to one subject; data from CF F508del/F508del samples are reported in bold; ↑subjects showing a percent increase of the GFP⁺ monocyte respect to pre; nd, not determined.

Table S4. Killing activity of PAO1-infected PBMC from CF pre, M1 and M6

pre	M1	M6
-126,42	**35,11**	**28,31**
-11,11	**44,58**	**19,63**
-7,69	30,01	17,24
-5,44	**32,51**	-0,36
-3,86	19,63	38,90
-3,70	**47,74**	**40,84**
-3,52	**25,49**	-0,61
-2,59	<u>nd</u>	-3,34
-0,21	**21,75**	**48,86**
1,99	nd	nd
2,91	**34,36**	**44,10**
8,52	41,42	37,65

Percentage reduction of viable bacteria recovered from PBMC infected with PAO1 as obtained by the intracellular killing assay. Negative results indicate intracellular bacterial growth rather than killing. Each row refers to one subject; homozygous F508del/F508del samples are reported in bold; nd, not determined.

Detailed methods

Bacteria. *P. aeruginosa* strains: laboratory strain PAO1; clonal clinical strains isolated from the same patient at the beginning of lung infection, AA2, and at the end of the lung disease, AA44; they are considered as representative of the early and late CF isolates, respectively (1). PAO1 was transformed with pUC30T-*gfpmut*3 plasmid (PAO1-GFP) and cultured in LB medium supplemented with 50 µg/mL gentamycin; the clinical isolates AA2 and AA44 were cultured in antibiotic-free LB medium. Cultures from frozen stocks were grown over night at 37°C with shaking (180 rpm), refreshed 1/10 in pre-warmed LB medium and grown to exponential phase ($OD_{600} \approx 0,5$). Bacteria were washed with PBS, resuspended in antibiotic-free cell-culture medium and used to infect PBMC samples at a MOI of 20.

PBMC isolation. Peripheral blood was collected by venipuncture into EDTA-vacutainers. PBMCs were isolated by density gradient centrifugation, collected, and washed three times with PBS supplemented with FBS 2% and EDTA 1mM. Subsequently, the cells were washed with PBS and resuspended in antibiotic-free RPMI supplemented with FBS 20% (10^6/mL) and used based on the experimental protocols. PBMC were depleted of CD14^{+} cells using anti-CD14 mAb coupled to

magnetic beads followed by immunomagnetic selection (Miltenyi Biotec, Bergisch Gladbach, Germany). The depletion, evaluated by staining with an anti-CD14 monoclonal antibody, was $\geq$ 90%.

Flow Cytometry. PBMCs were washed twice with PBS and incubated with conjugated human monoclonal anti-CD14 or isotype control antibodies in the dark for 20 min on ice. After incubation, cells were washed and freshly analyzed. The analysis was performed as follow: i) forward and side scatter plots; ii) monocytes based on FSC-SSC were gated; iii) percentages of positivity to anti-CD14 antibody. The range of events analyzed was 10.000-100.000. CellQuest and FlowJo softwares were used for sample collection and data analysis, respectively.

Phagocytosis Assay by Flow Cytometry. PBMCs (5×10^5) were infected with PAO1-GFP at a MOI of 20 for 30 min. at 37°C in 5% CO_2. When applied, cells were pre-treated with 10 μM Cytochalasin B for 30 min. At the end of infection, PBMCs were gently washed twice with PBS and analyzed by flow cytometry as described above. Phagocytosis was evaluated as the percentage of GFP^+ events calculated on the non-infected cutoff. Additionally, to evaluate the possible phagocytosis activity of PBMC cells other than monocytes, GFP positivity was also evaluated in the other PBMC populations.

PBMCs Infection and Analysis of Bacterial Uptake and Intracellular Killing. 5×10^5 of freshly isolated PBMCs were infected with *P. aeruginosa* strains. When applied, PBMCs were pretreated with DPI (10 μM, for 30 min at 37°C in 5% CO_2). Infection was synchronized by centrifugation and the infected cells were then incubated at 37°C in 5% CO_2 for 30 min. At the end of the infection, cells were treated with antibiotics (amikacin and ceftazidime, 1 mg/mL each) at 37°C for 15 min, to eliminate non-phagocytosed bacteria. Afterwards, the infected cells were washed twice and recovered in PBS for the analysis of bacterial uptake or in culture medium to evaluate the microbicidal activity. For the latter, cells were incubated for 60 min at 37°C and 5%CO2 in culture medium supplemented with sub-inhibitory concentration of antibiotics (0.1 mg/mL each). CFUs at the end of infection (t_0) and one hour after infection (t_{60}) were determined by plating aliquots in LB plates.

Bactericidal activity was calculated as follows: $(CFU_{t0} - CFU_{t60}) / CFU_{t0} \times 100$.

Additionally, bacterial killing of PBMC was calculated with linear regression model to determine the slope values of killing curves.

ROS Measurement. Luminol probe was used to measure intracellular O_2^- levels as described in Cavinato *et al*., 2020 (2) with minor modifications. Briefly, PBMC, pretreated or not with DPI (10 μM, for 30 min at 37°C in 5% CO_2) were resuspended in HBSS without phenol red supplemented with luminol, 25μg/mL. 5×10^5 cells/well were seeded in white 96-well plates and infected with *P. aeruginosa* at a MOI of 20. The chemiluminescence was measured every 10 min up to 120 min with the multilabel counter CLARIOstar PLUS (BMG LABTECH). The data were corrected based on the controls without PBMC. Quantitative analysis of O_2^- production was performed by determination of the area under the curve (AUC) using the GraphPad Prism software.

ROS measurement by the H2DCFDA probe was performed according to the supplier's specification. Briefly, PBMC (5×10^5) were resuspended in HBSS without phenol red, seeded in black 96-well plate and infected with *P. aeruginosa* for 30 min 37°C in 5% CO_2. Subsequently, cells were load with H2DCFDA (10 μM) probe for further 30 min and gently washed with HBSS without phenol red. Fluorescence was measured (excitation 495/absorption 525 nm) with the multilabel counter. DPI-treated controls were included. Data were corrected on the uninfected controls.

Western Blots. Monocytes were isolated by negative selection using EasySep monocyte enrichment kit without CD16 depletion, following the manufacturer's specifications. Collected cells were incubated in complete culture medium without antibiotics and infected with PAO1 at a MOI=20 for 30 min at 37°C in 5% CO2. Non-infected controls were also included. After infection, cells were treated with antibiotics, gently washed twice and finally lysed in HEPES 50 mM, NaCl 150 mM, EGTA 10 mM, NP-140 1%, NaF 100 mM, Na3VO4 8 mM, Glycerol 5%, Pefabloc 2 mM, proteinase cocktail inhibitor. Western Blots were performed with 30 μg of proteins according to Mecocci *et al*., 2020 (3). Membranes were blocked with 5% skimmed milk, in PBS-Tween 20 (0,1%) or 5% BSA in TBS-Tween 20 (0,1%) and stained with primary and secondary antibodies (Supplementary Table 1).

Cytokine quantification. Cytokine quantification was performed as previously reported (4) in supernatants of monocytes untreated or treated for 18 hr with *P. aeruginosa* LPS, 500 ng/ml, in culture medium supplemented with low endotoxin FBS 2%.

Supplementary References

1. Cigana C, Curcurù L, Leone MR, Ieranò T, Lorè NI, Bianconi I, Silipo A, Cozzolino F, Lanzetta R, Molinaro A, Bernardini ML, Bragonzi A. Pseudomonas aeruginosa exploits lipid A and muropeptides modification as a strategy to lower innate immunity during cystic fibrosis lung infection. *PLoS One*. 2009;4:12.

2. Cavinato L, Genise E, Luly FR, Di Domenico EG, Del Porto P, Ascenzioni F. Escaping the Phagocytic Oxidative Burst: The Role of SODB in the Survival of Pseudomonas aeruginosa Within Macrophages. *Front Microbiol* 2020;11:326.

3. Mecocci S, Gevi F, Pietrucci D, Cavinato L, Luly FR, Pascucci L, Petrini S, Ascenzioni F, Zolla L, Chillemi G, Cappelli K. Anti-Inflammatory Potential of Cow, Donkey and Goat Milk Extracellular Vesicles as Revealed by Metabolomic Profile. *Nutrients* 2020;12.

4. Luly FR, Lévêque M, Licursi V, Cimino G, Martin-Chouly C, Théret N, Negri R, Cavinato L, Ascenzioni F, Del Porto P. MiR-146a is over-expressed and controls IL-6 production in cystic fibrosis macrophages. *Sci Rep* 2019;9:16259.